Non-invasive method of melanoma detection on the skin surface through extraction of image features using modified CAT optimization algorithm

N. Prabhakaran*

Department of Electronics and Communication, Aalim Muhammed Salegh College of Engineering, I.A.F., Avadi, Chennai 600 055, India

In this study, melanoma was detected at an early stage using modified CAT optimization algorithm (MCOA) based on non-convex boundary edge extraction, pixel size, shape and intensity variations on the skin. MCOA can detect skin cancer at an early stage by extracting the non-convex border of the affected region prevent cancer spread. Thus melanoma is curable when detected at an early stage. MCOA extracts image features and obtains non-convex boundaries of melanoma in the skin image. The non-convex boundary region leads to visualization of discriminative features of melanoma based on the region of interest and scaling. The proposed MCOA delineates the affected region through non-convex border extraction and edge detection. An accuracy of 85% was obtained in the detection of melanoma using MCOA, when compared to traditional algorithms.

Keywords: Contour refinement, edge detection, melanoma, non-convex boundary, optimization algorithm.

Melanoma detection and optimization algorithm

IN India, the mortality rate of skin cancer patients increases by 25% every year[1]. Melanoma disease detection at an early stage depends on the expertise of the radiologist/oncologist. Melanoma is a skin cancer which is diagnosed through skin lesions in the images[2]. The lesion appears in irregular shape and boundary, and requires an efficient enhanced algorithm for visual identification from the image[3]. The skin lesion is extracted from the image based on colour, texture, shape and pixel intensity. The region of interest (ROI)-based skin lesions is clustered to extract the discriminative features for melanoma detection[4]. In clinical diagnosis, skin lesions less than 6 mm in diameter are not detected and rely on skin prick tests for melanoma diagnosis. This test examines only the surface of the skin and not below. The surface of skin is analysed through image segmentation and skin image with low contrast leads to inaccurate diagnosis[5]. The OTSU method segments the skin lesion region from the image with less accuracy. The particle swarm optimization (PSO) algorithm is used to detect morphological changes in the skin through size, shape, colour and texture feature extraction from the image[6]. The extracted features are used for the detection of melanoma. Decomposition of melanoma image with filter removes artefacts and enhances the contrast. The filtered images have illumination variation in the lesion region and improve the prediction of melanoma[7]. The skin lesions classification is performed through feature extraction and histogram analysis. The histogram analysis is based on the shape, colour and pixel intensity of the lesion region. The segmentation algorithm extracts the lesion boundary, performs feature analysis and improves the visualization of the lesion[8]. Automatic detection of melanoma is done through three main stages. In the initial stage, the lesion image is automatically segmented to determine the lesion area with accuracy. In the second stage, the physical features of the lesion from the image are extracted. In the final stage, the extracted features are used for the diagnosis of lesions and to predict melanoma[9]. Skin cancer lesion prediction from image segmentation algorithm has maximum accuracy[10]. The proposed modified CAT optimization algorithm (MCOA) differentiates images such as benign, melanoma and malignant through accurate edge enhancement and extraction. The existing algorithms such as segmentation, enhancement and histogram-based analysis do not segment skin lesion and discontinuity in edge is seen in skin lesion. The proposed MCOA highlights the non-convex border region of skin lesions and extracts features for the detection of skin cancer. The different texture features are delineated for early detection of skin cancer.

Literature survey

Fuzzy *c*-means clustering algorithm has been proposed to classify and detect skin lesions accurately. It performs better than traditional clustering algorithms. The skin lesion classification can also be done using deep learning algorithms[11]. Automatic detection of skin lesions using YOLOv4 is highly correlated with the non-infected and infected regions, and improves the accuracy of melanoma prediction.

*e-mail: captainprabhakar1982@yahoo.co.in

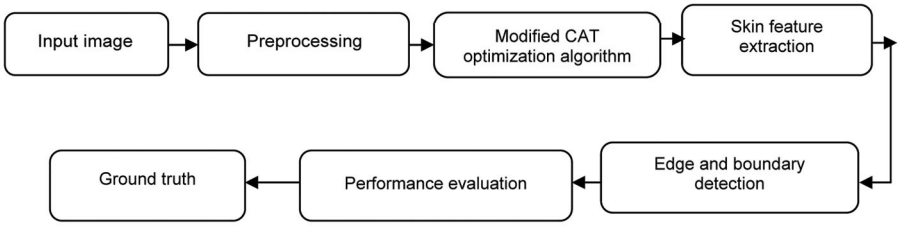

Figure 1. Methodology diagram of melanoma detection at earlier stage using modified CAT optimization algorithm.

Melanoma is detected from skin lesions using DarkNet and contour edge detection. Melanoma skin segmentation is done through skin enhancement to detect melanoma cells accurately. Finally, segmentation of the melanoma cell region is done using YOLOv4 (ref. 12). The segmented lesion in the image is analysed using the ABCD rule. Physicians detect melanoma in the image after enhancing the skin lesion, which has irregular borders and colour variation[13]. A low-power radar with a frequency of 77 GHz is used for skin cancer detection through imaging. It differentiates melanoma and normal skin based on the dielectric properties of the tissue with high accuracy (microns). A low-power radar method consists of six port interferometer. This is a low-cost method to detect skin cancer[14]. The ROI segmentation with the *k*-means clustering algorithm extracts melanoma cells[15]. Early detection of a skin lesion using the deep learning method is time-consuming and requires high computational complexity than the ensemble method. The deep learning methods such as SegNet and U-Net perform better than other deep learning architectures such as ReNet, and Google Net[16]. Skin diseases are analysed using the transfer learning method after fine-tuning the image to improve the cancer detection accuracy[17]. Melanoma detection using a neural network system is trained with pre-samples of the network using the perception model. The histogram gradient coupled with the ABCD rule extracts low-level features in the image such as texture, shape, colour and pixel intensity. The above method extracts the features and enhances the accuracy of skin lesion image[18]. Melanoma is detected from the pigmented lesion and the probability of false pixels in the image. The above method differentiates the object of pigmentation from benign cancer tissues[19]. A fast and accurate method of skin lesion detection is performed through probes in frequency range of 40 GHz. Melanoma detection was simulated using CST MICROWAVE STUDIO for earlier detection[20]. Melanoma classification using the convolution neural network has better prediction accuracy. The CNN method has been compared with traditional methods for delineation of melanoma region[21]. Skin lesion image classification improves the performance of melanoma detection at an early stage through the image augmentation method, and an accuracy of melanoma detection is about 90% through augumentation[22]. The pixel-wise class imbalance arises during skin segmentation due to fewer cancer pixels and pixel intensity. The Jaccard method outperforms the traditional algorithms, which performs the classification and segmentation. Traditional methods reduce the loss function and performance of melanoma detection is less[23]. Hair removal from the skin region and segmentation of the skin are critical tasks for physicians. For hair removal from the lesions, the encoder–decoder method has been developed. This method overcomes the problem of reduced loss function during the segmentation. Accuracy in delineation after removal of skin and hair is performed through deep learning method[24]. Deep learning method extracts the background in the lesion images, detects melanoma through light-weight segmentation of the lesion area and visualizes the melanoma features through using size, shape and pixel intensity[25]. In MCOA, non-convex border in the images is optimized, and it extracts features by boundaries and edges of the cancer region and identifies different types of skin cancer. MCOA delineates the skin cancer region through the non-convex border for melanoma detection and the detection of different stages such as benign, melanoma and nevus images.

Methodology

The CAT optimization algorithm extracts image features for early detection of melanoma and helps radiologists in the diagnosis of skin cancer. Figure 1 shows the proposed block diagram for melanoma detection at an early stage. MCOA segments the skin lesion from images and validates through ground-truth verification and improves the diagnosis of skin cancer at an early stage. The algorithm detects the edges and boundaries of the melanoma region on the image. It achieves better results when compared to the existing algorithms, and validates through accuracy, sensitivity, specificity and precision. The ground-truth verification is performed through measurement of true boundaries after processing the skin image with MCOA algorithm. The datasets for this study were taken from the repository of the Royal Mother Hospital, Chennai, India which contains 2000 images as well as a standard dataset which is openly available (HAM10000). The standard dataset has benign, keratosis lesions, melanoma and nevus images. The test data were taken from ISBI 2021[72] and PH1[44] with eight-bit RGB colour images with a resolution of 560 × 560 pixels, which consist of 250 dermoscopic images of skin lesions.

In CAT optimization algorithm, trace and seek mode were tuned based on the melanoma pixel size, texture and intensity. For example, trace and seek mode in CAT optimization algorithm increase with cost function for enhancement of high-frequency component pixel and for low-frequency component pixel enhance through tuning the seek mode.

Pre-processing

The pre-processing of melanoma images differentiates contours and removes artefacts. The median filter algorithm enhances the melanoma pixels. The pre-processing of images through median filter is more suitable for MCOA-based melanoma region segmentation.

Skin feature extraction

The melanoma region in the skin images was segmented and performance evaluation was done through statistical values obtained from the output image. The similarity index determines the quality of the skin lesion image and accuracy is analysed through PSNR. Features extracted using MCOA provide enhanced non-convex borders. The quality of the images was retained in the output image after processing with MCOA. PSNR evaluates the quality of the extracted regions processed with MCOA, and this algorithm improves accuracy in melanoma detection. PSNR is estimated as follows

$$\text{PSNR} = -20 * \log_{10}\text{SL/MSE}, \quad (1)$$

where MSE is the mean square error and SL is the skin lesion.

The feature extracted from skin lesion through MCOA removes the noise factor and identifies the clear spread of cancer cells.

Region of interest

ROI in skin lesion extracts the edges and boundaries of cancer cells with respect to cancer pixel size, shape and intensity on the skin image. Multiple features in the skin help in the detection of skin cancer at an early stage. The infected, non-infected and spreading areas of cancer are extracted through ROI, obtained through segmentation of MCOA and used for cancer spread detection. The melanoma-infected areas are measured through the non-convex border features from MCOA output images. MCOA-based ROI classifies melanoma detection at an early stage through segmentation of melanoma regions through seek mode and trace mode in MCOA.

Edge and boundary detection of skin lesion images: The melanoma-infected area is segmented using MCOA and the non-convex boundary region in the image and its features are extracted. The edges are detected and optimized through MCOA and the image feature is extracted through boundary regions of cancer cells for early detection. MCOA differentiates the image features through seek and trace modes. This is based on the smoothing effect, particularly in the melanoma region. In traditional optimization algorithms, weights are associated with particular pixel region-based extraction. MCOA differentiates the affected and non-affected areas in the skin images at an early stage through the enhancement of boundaries and edges of the melanoma region on the skin surface. The differentiation of melanoma through MCOA is based on the non-convex borders of cancer-affected regions.

Threshold segmentation algorithm for noise and noiseless images: In MCOA, the population starts with seeking mode and tracing mode; threshold selection is based on the variables. MCOA clusters the possible solutions to be optimized in the pixel range from false positive to false negative. The fitness solution for each optimization fixes the best solution into the solution space and optimizes the pixels. CAT moves towards the optimal area by updating its position and velocity with fewer iterations, which highly depends on the non-convex border in the solution space. CSO optimizes through the best threshold value for each solution, and classifies the pixel set with a false negative and false positive. The threshold values are detected by optimization of the clusters through the non-convex border in the solution space at each level of iteration.

Skin cancer detection using MCOA

MCOA optimizes both the inner and outer boundaries of melanoma regions in the images for early detection of cancer. The algorithm optimizes through seeking mode and tracing mode, enhances the pixel intensity of cancer cells with respect to false positive and false negative pixels in the skin lesion image, and enhances edges and boundaries. MCOA-based pixel region intensity in the output image increases by 7% in the melanoma region, which leads to the detection of different types of skin cancers such as benign, malignant and nevus.

Results and discussion

Figure 2 shows the skin lesion images for early diagnosis. Figure 2 *a* shows the input image with melanoma, while Figure 2 *j* and *k* shows the MCOA processed images of skin lesion of size 62.24 mm. MCOA extracts pixel intensity with low resolution. In MCOA, the neighbouring pixels are used for prediction of melanoma in the image more accurately. The predicted pixels match the cancer images of other datasets and detect skin cancer. The lesion image is marked with a ruler and spread of infection is measured.

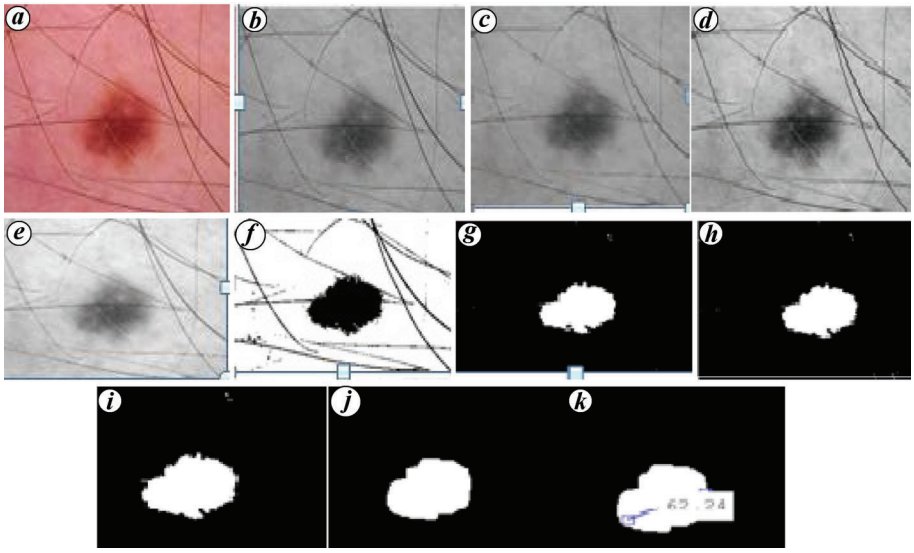

Figure 2. Skin lesion images and extraction of melonama to benign stages. ***a***, Input image; ***b***, Raw image; ***c***, Image with noise; ***d***, Noiseless image; ***e***, Background change in image; ***f***, Destroyed; ***g***, Change in background of image; ***h***, Holes filled; ***i***, Remove blob in the image; ***j***, Remove small blobs in the image; ***k***, Threshold detection.

Table 1. Statistical parameters of skin lesion image – benign stage

	Nevus			Melanoma			SK			Overall		
Method	SEN	SPE	ACCESS	SEN	SPE	ACCESS	SEN	SPE	ACCESS	SEN	SPE	ACCESS
MCSO-2	78.34	82.76	85.40	80.50	81.26	85.98	70.11	74.50	87.46	77.66	92.40	90.80
MCSO-4	80.67	92.20	90.59	81.56	88.80	85.86	70.58	78.96	89.20	80.10	95.28	92.65
MCSO-6	82.45	94.70	92.68	82.70	90.41	87.25	73.89	80.52	92.54	82.41	96.76	94.45
MCSO-8	85.54	96.61	93.45	85.98	93.74	90.46	77.74	84.93	94.74	83.65	97.32	96.35
MCSO-10	88.76	97.80	95.28	88.95	96.43	93.59	80.85	87.96	96.85	85.96	98.45	97.65
MCSO-12	90.58	98.48	97.46	91.85	98.74	95.58	85.85	92.72	98.96	89.42	98.78	98.45
MCSO-14	92.85	98.89	98.78	95.15	99.20	97.86	89.58	96.74	99.24	95.85	99.27	99.54

SEN, Sensitivity; SPE, Specificity, MCSO, Modified CAT optimization algorithm.

MCOA enhances the image and compares it with the input image for ground-truth verification. The result is validated and statistical measurements are performed; the accuracy of cancer detection is about 85.60%. MCOA optimizes skin lesion in the image through the seeking mode and tracing mode. It outperforms traditional algorithms such as fuzzy c-means clustering algorithm, genetic algorithm and particle swarm optimization algorithm in terms of accuracy and complexity. MCOA has better accuracy, less computational time and less iteration. Figure 2 shows the skin lesion images and extraction of melanoma at the benign stage.

Performance evaluation

MCOA measures parameters such as similarity index, coefficient, sensitivity, specificity and accuracy. The correlation coefficient is linked with skin lesion images for extraction of the non-convex cancer region in image. All the parameters were determined with the total number of pixels after processing with MCOA. The algorithm classifies false pixels and converts them into true pixels, enhancing the image with high accuracy for the cancer region. MCOA results are validated and predict the prognosis of skin lesion. Equations (2)–(5) show the sensitivity, specificity, accuracy and JSI.

$$\text{Sensitivity} = \text{TP/TP} + \text{FN}, \tag{2}$$

$$\text{Specificity} = \text{TN/FP} + \text{TN}, \tag{3}$$

$$\text{Accuracy} = \text{TP} + \text{TN/TP} + \text{FP} + \text{TN} + \text{FN}, \tag{4}$$

$$\text{JSI} = \text{TP/TP} + \text{FP} + \text{FN}. \tag{5}$$

where TP is the true positive, FN the false negative, FP the false positive and TN is the true negative.

Table 1 shows the performance evaluation of different stages of melanoma. Figure 3 shows compares the sensitivity and accuracy of benign melanoma images.

Figure 4 depicts melanoma images at stage I. The melanoma is 147.14 mm in size and the skin lesion region with pixel intensity of low resolution was extracted using MCOA.

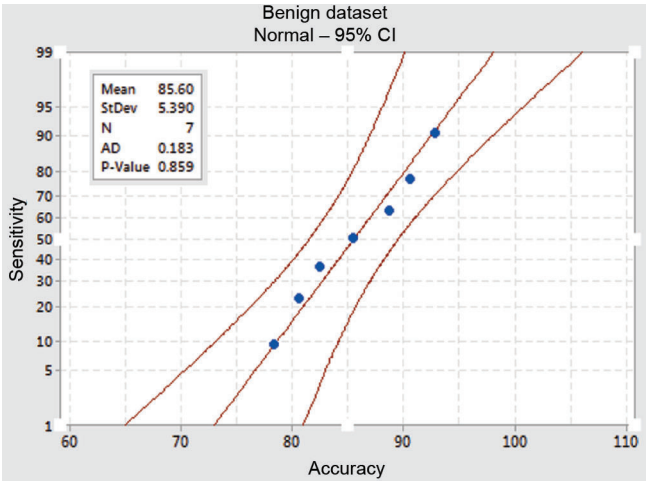

Figure 3. Relationship between accuracy, sensitivity and specificity of skin lesion images for a benign condition.

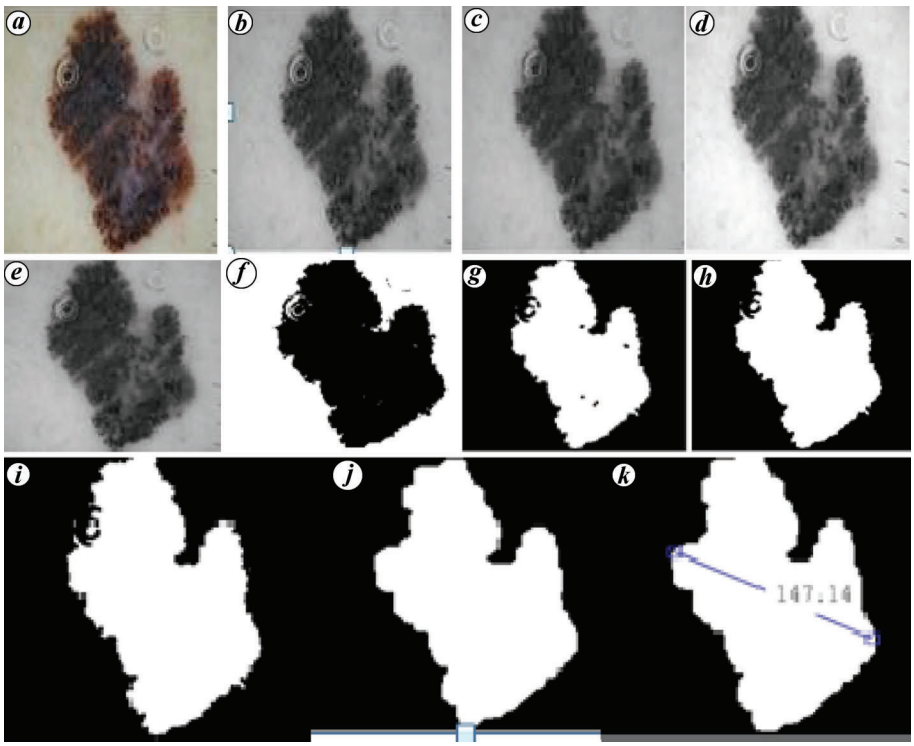

Figure 4. Dataset of skin lesion images for extraction of melanoma (stage I). ***a***, Input image; ***b***, Raw image; ***c***, Image with noise; ***d***, Noiseless image; ***e***, Background change in skin image; ***f***, Destroyed edges in the skin image; ***g***, Change in background of skin image; ***h***, Holes filled; ***i***, Remove blob in the skin image; ***j***, Remove small blobs in the skin image; ***k***, Threshold detection.

Table 2. Statistical parameters of the dataset of skin lesion image – melanoma

Method	Initial stage			I stage			II stage			III stage		
	SEN	SPE	ACC	SEN	SPE	ACC	SEN	SPE	ACC	SEN	SPE	ACC
MCSO-2	80.70	78.45	75.30	76.80	85.95	90.20	89.55	75.68	77.54	85.20	70.25	85.11
MCSO-4	82.52	80.59	77.59	78.58	87.96	91.97	92.56	77.85	79.65	86.48	72.96	86.85
MCSO-6	83.55	82.85	79.46	80.63	89.48	92.39	94.43	80.35	82.58	88.36	75.52	89.45
MCSO-8	85.93	84.59	82.65	83.59	93.55	95.44	95.65	83.24	86.14	90.65	78.66	91.78
MCSO-10	87.45	86.46	85.65	84.65	95.14	96.75	97.53	85.51	90.86	93.47	83.78	94.96
MCSO-12	89.15	90.65	87.95	88.42	97.23	98.12	98.52	87.65	94.85	96.45	85.15	96.92
MCSO-14	93.48	92.58	94.86	93.49	98.64	99.99	99.48	95.45	96.48	98.35	88.66	98.56

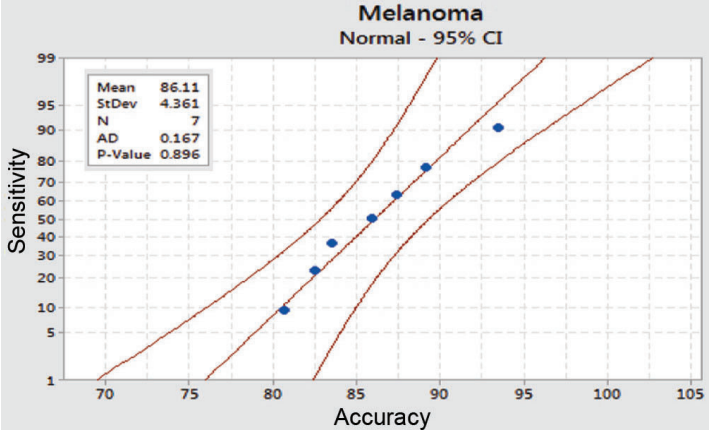

Figure 5. Relationship between accuracy and sensitivity of skin lesion images for melanoma (stage I).

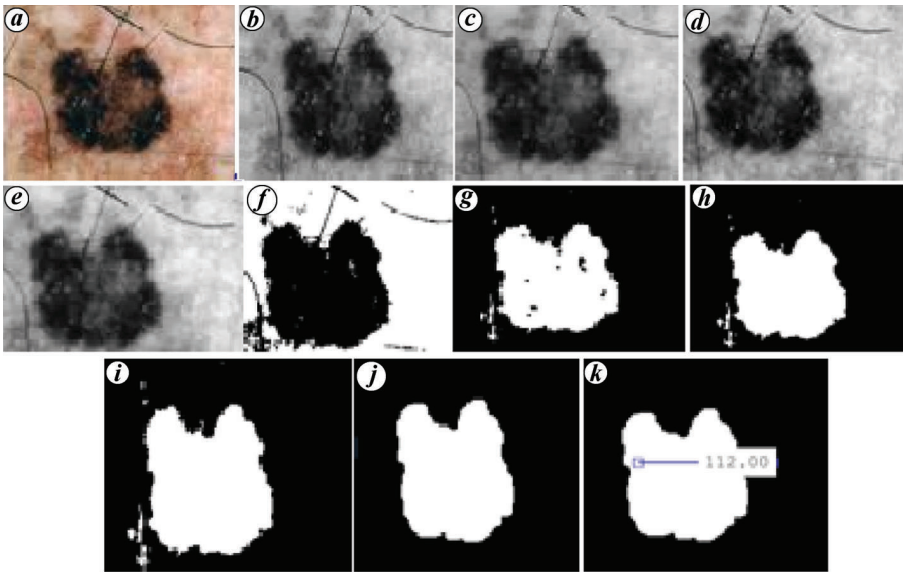

Figure 6. Dataset of skin lesion images for extraction of melanoma (stage II). ***a***, Input image; ***b***, Raw image; ***c***, Image with noise; ***d***, Noiseless image; ***e***, Background change in the skin image; ***f***, Destroyed edges in the skin image; ***g***, Change in background of skin image; ***h***, Holes filled; ***i***, Remove blob in the skin image; ***j***, Remove small blobs in the skin image; ***k***, Threshold detection.

To predict disease at an earlier stage, high-intensity and low-intensity pixles are delineated. The low- and high-intensity pixels show the spread on the cancer on the skin surface. The skin lesion image is enhanced by MCOA and compared with the ground-truth image. Figure 4 shows the melanoma image (stage I) processed with MCOA; the accuracy is about 86.11%.

Table 2 shows the statistical parameters of the dataset of skin lesion images in stage I.

Figure 5 shows the relationship between accuracy and sensitivity of melonoma images in stage I skin.

For early diagnosis, melanoma images were processed with MCOA. The images are of melanoma stage III and MCOA processed image has 112 mm of cancer cells (Figure 4 *k*). From the input image, the pixel intensity of low-resolution images is extracted. The low-frequency pixel and neighbouring pixels are used for early detection of melanoma at stage III.

Figure 6 shows melanoma images in stage II processed with MCOA. Table 3 shows statistical parameters of melanoma images in stage II. Figure 7 shows the relationship between accuracy, sensitivity and specificity of skin lesion images.

The lesion images after processed with MCOA algorithm, non-convex borders are enhanced and algorithm optimizes the true positive pixels and true negative pixels. MCOA optimizes the edges of skin lesion through tracking mode and seeking mode method in the MCOA algorithm for better segmentation and enhancement of the edges and boundary in the melanoma images. Table 4 shows the performance of skin lesion images with and without optimization. It can be observed from table that when using

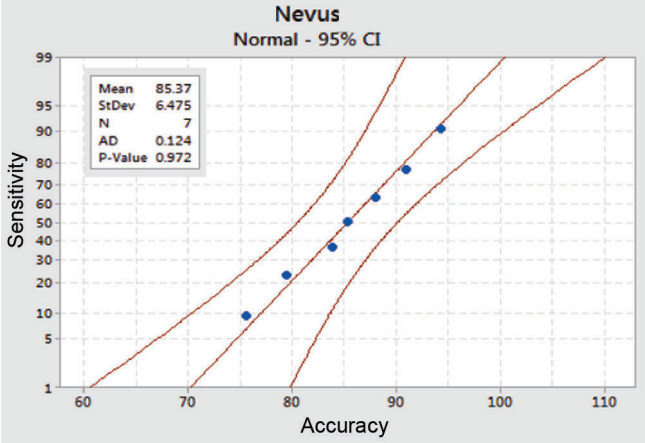

Figure 7. Relationship between accuracy, sensitivity and specificity of skin lesion images for nevus disease.

Table 3. Statistical parameters of the melanoma image in stage II

	Initial stage			I stage			II stage			III stage		
Method	SEN	SPE	ACC	SEN	SPE	ACC	SEN	SPE	ACC	SEN	SPE	ACC
MCSO-2	75.56	75.85	83.85	74.12	80.77	76.58	89.45	90.12	87.15	82.63	80.15	75.12
MCSO-4	79.51	79.62	85.74	79.12	85.69	79.98	90.78	92.86	90.74	85.16	83.59	79.15
MCSO-6	83.85	85.96	87.15	83.74	86.98	83.96	93.95	94.75	93.35	89.85	87.96	82.14
MCSO-8	85.36	87.45	90.98	85.75	90.85	86.75	95.36	96.68	95.35	93.25	90.69	85.78
MCSO-10	87.98	90.45	93.15	87.12	93.45	89.54	97.45	97.62	96.74	95.78	93.96	89.15
MCSO-12	90.96	93.45	94.12	93.85	96.75	93.62	98.85	98.45	97.69	97.12	95.75	93.08
MCSO-14	94.35	96.15	97.96	97.94	99.72	96.37	99.81	99.30	98.64	99.50	97.68	96.82

Table 4. Performance with and without optimization in the skin lesion images

	Melanoma (with optimization) MCOA			Melanoma (without optimization)		
Method	SEN	SPE	ACC	SEN	SPE	ACC
MCSO	78.98	72.92	75.60	32.18	30.62	31.28
MCSO	80.32	75.32	77.32	40.11	32.12	34.28
MCSO	83.94	77.98	80.65	41.28	32.33	40.22
MCSO	87.96	80.98	82.64	42.28	40.28	40.11
MCSO	90.63	84.75	85.70	45.00	41.23	41.28
MCSO	93.54	85.12	89.20	45.00	42.11	40.18
MCSO-14	96.87	89.06	95.21	42.18	40.18	41.28

Table 5. Comparison of various optimization algorithms

Skin image	Fuzzy *c*-means clustering (%)			Genetic algorithm (%)			MCO (%)		
Initial	61	71	70	53	56	69	83	85	84.5
First	67	72	70	71	70	68	87	85	85
Second	67	76	71	67	78	68	85	83	85

MCOA, the accuracy of extraction of skin cancer at an early stage is about 70%–80%, while without optimization the accuracy is about 45%–50%. The accuracy of MCOA is due to size, shape and enhanced non-convex borders in the lesion region.

MCOA was compared with the fuzzy *c*-means clustering algorithm and genetic algorithm. High accuracy was achieved with MCOA for detecting skin cancer at an early stage, when compared with the other algorithms. Table 5 shows a comparison of various optimization algorithms.

Conclusion

Recent developments in cancer treatments can help cure melanoma, when detected early. MCOA detects the

non-convex borders using tracing and seeking mode. The proposed algorithm improves melanoma detection at an earlier stage after the removal of artefacts such as noise and hair or tiny blood vessels in the skin image. The results demonstrate that the proposed MCOA-based melanoma detection outperforms the other traditional methods. This method shows enhanced non-convex borders, and the spreading of cancer cells is detected at an early stage. MCOA algorithm can be used for tuning deep learning algorithms and improve the prediction accuracy of melanoma.

1. Siegel, R. L., Miller, K. D., Fuchs, H. E. and Jemal, A., Cancer statistics. *CA: Cancer J. Clin.*, 2021, **71**, 7–33; doi:10.3322/caac.21654.
2. Petrie, T., Samatham, R., Witkowski, A. M., Esteva, A. and Leachman, S. A., Melanoma early detection: big data, bigger picture. *J. Invest. Dermatol.*, 2019, **139**(1), 25–30; doi:10.1016/j.jid.2018.06.187.
3. Narayanamurthy, V. *et al.*, Skin cancer detection using non-invasive techniques. *RSC Adv.*, 2018, **49**, 28095–28130; doi:10.1039/c8ra04164d.
4. Olugbara, O. O., Taiwo, T. B. and Heukelman, D., Segmentation of melanoma skin lesion using perceptual color difference saliency with morphological analysis. *Math. Probl. Eng.*, 2018; doi:10.1155/2018/1524286.
5. Masood, A. and Al-Jumaily, A. A., Computer-aided diagnostic support system for skin cancer: a review of techniques and algorithms. *Int. J. Biomed. Imag.*, 2013; doi:10.1155/2013/323268.
6. Dey, N., Rajinikanth, V., Ashour, A. S. and Tavares, J. M. R. S., Social group optimization supported segmentation and evaluation of skin melanoma images. *Symmetry*, 2018; doi:10.3390/sym10020051.
7. Saba, T., Recent advancement in cancer detection using machine learning: systematic survey of decades, comparisons and challenges. *J. Infect. Public Health*, 2020, **13**, 1274–1289; doi:10.1016/j.jiph.2020.06.033.
8. Rout, R., Parida, P., Alotaibi, Y., Alghamdi, S. and Khalaf, O. I., Skin lesion extraction using multiscale morphological local variance reconstruction based watershed transform and fast fuzzy *c*-means clustering. *Symmetry*, 2021, **13**(11), 2085; doi:10.3390/sym13112085.
9. Javed, R., Rahim, M. S. M., Saba, T. and Rehman, A., A comparative study of features selection for skin lesion detection from dermoscopic images. *Netw. Model. Anal. Health Informat., Bioinformat.*, 2020, **9**; doi:10.1007/s13721-019-0209-1.
10. Pereira, P. M. M. *et al.*, Dermoscopic skin lesion image segmentation based on local binary pattern clustering: comparative study. *Biomed. Signal Process. Control*, 2020, **59**, 101924; doi:10.1016/j.bspc.2020.101924.
11. Adegun, A. and Viriri, S., FCN-based DenseNet framework for automated detection and classification of skin lesions in dermoscopy images. *IEEE Access*, 2020, **8**, 150377–150396; doi:10.1109/ACCESS.2020.3016651.
12. Albahli, S., Nida, N., Irtaza, A., Yousaf, M. H. and Mahmood, M. T., Melanoma lesion detection and segmentation using YOLOv4-DarkNet and active contour. *IEEE Access*, 2020, **8**, 198403–198414; doi:10.1109/access.2020.3035345.
13. Ali, A. R. H., Li, J. and Yang, G., Automating the ABCD rule for melanoma detection: a survey. *IEEE Access*, 2020, **8**, 83333–83346; doi:10.1109/ACCESS.2020.2991034.
14. Arab, H., Chioukh, L., Dashti Ardakani, M., Dufour, S. and Tatu, S. O., Early-stage detection of melanoma skin cancer using contactless millimeter-wave sensors. *IEEE Sens. J.*, 2020, **20**(13), 7310–7317; doi:10.1109/JSEN.2020.2969414.
15. Ashraf, R. *et al.*, Region-of-interest based transfer learning assisted framework for skin cancer detection. *IEEE Access*, 2020, **8**, 147858–147871; doi:10.1109/ACCESS.2020.3014701.
16. Gan, K. B., Chong, K. S., Nawoor, A. D., Then, S. M., Abdul Murad, N. A. and Jamal, A. R. A., Development of an HLA-B*58:01 allele screening system for allopurinol-induced severe cutaneous adverse reactions detection. *IEEE Access*, 2020, **8**, 225306–225323; doi:10.1109/ACCESS.2020.3044562.
17. Goyal, M., Oakley, A., Bansal, P., Dancey, D. and Yap, M. H., Skin lesion segmentation in dermoscopic images with ensemble deep learning methods. *IEEE Access*, 2020, **8**, 4171–4181; doi:10.1109/ACCESS.2019.2960504.
18. Gu, Y., Ge, Z., Bonnington, C. P. and Zhou, J., Progressive transfer learning and adversarial domain adaptation for cross-domain skin disease classification. *IEEE J. Biomed. Health Informat.*, 2020, **24**(5), 1379–1393; doi:10.1109/JBHI.2019.2942429.
19. Ichim, L. and Popescu, D., Melanoma detection using an objective system based on multiple connected neural networks. *IEEE Access*, 2020, **8**, 179189–179202; doi:10.1109/access.2020.3028248.
20. Kelman, Y. T., Yitzhak, H. L., Shabairou, N., Finder, S. and Zalevsky, Z., Multi-spectral optimization for tissue probing using machine learning. *IEEE Photon. J.*, 2021, **13**(1); doi:10.1109/JPHOT.2020.3048015.
21. Mansutti, G., Mobashsher, A. T., Bialkowski, K., Mohammed, B. and Abbosh, A., Millimeter-wave substrate integrated waveguide probe for skin cancer detection. *IEEE Trans. Biomed. Eng.*, 2020, **67**(9), 2462–2472; doi:10.1109/TBME.2019.2963104.
22. Naeem, A., Farooq, M. S., Khelifi, A. and Abid, A., Malignant melanoma classification using deep learning: datasets, performance measurements, challenges and opportunities. *IEEE Access*, 2020, **8**, 110575–110597; doi:10.1109/ACCESS.2020.3001507.
23. Pham, T. C., Doucet, A., Luong, C. M., Tran, C. T. and Hoang, V. D., Improving skin-disease classification based on customized loss function combined with balanced mini-batch logic and real-time image augmentation. *IEEE Access*, 2020, **8**, 150725–150737; doi:10.1109/ACCESS.2020.3016653.
24. Song, L., Lin, J., Wang, Z. J. and Wang, H., An end-to-end multi-task deep learning framework for skin lesion analysis. *IEEE J. Biomed. Health Informat.*, 2020, **24**, 2912–2921; doi:10.1109/JBHI.2020.2973614.
25. Talavera-Martinez, L., Bibiloni, P. and Gonzalez-Hidalgo, M., Hair segmentation and removal in dermoscopic images using deep learning. *IEEE Access*, 2021, **9**, 2694–2704; doi:10.1109/ACCESS.2020.3047258.

ACKNOWLEDGEMENT. I thank Prof Dr N. R. Shanker (Computer Science and Engineering Department, Aalim Muhammed Salegh College of Engineering, I.A.F., Avadi, Chennai, for his expertise and assistance throughout all aspects of the study and his help in rewriting the manuscript after review comments.

Received 7 October 2021; re-revised accepted 4 May 2022

doi: 10.18520/cs/v124/i5/562-569